Graphene/h-BN/ZnO van der Waals tunneling heterostructure based ultraviolet photodetector

Zhiqian Wu,[1] Xiaoqiang Li,[1, 2] Huikai Zhong,[1]Shengjiao Zhang,[1, 2] Peng Wang,[1, 2] Tae-ho Kim,[3] Sung Soo Kwak,[3] Cheng Liu,[2] Hongsheng Chen,[1, 2] Sang-Woo Kim,[3,*] and Shisheng Lin,[1, 2,*]

[1]*Department of Information Science and Electronic Engineering, Zhejiang University, Hangzhou 310027, China*
[2]*State Key Laboratory of Modern Optical Instrumentation, Zhejiang University, Hangzhou, 310027, China*
[3]*School of Advanced Materials Science and Engineering, SKKU Advanced Institute of Nanotechnology (SAINT), Center for Human Interface Nanotechnology (HINT), SKKU-Samsung Graphene Center, Sungkyunkwan University (SKKU), Suwon 440-746, South Korea*
[3]*kimsw1@skku.edu*
[*]*shishenglin@zju.edu.cn*

Abstract: We report a novel ultraviolet photodetector based on graphene/h-BN/ZnO van der Waals heterostructure. Graphene/ZnO heterostructure shows poor rectification behavior and almost no photoresponse. In comparison, graphene/h-BN/ZnO structure shows improved electrical rectified behavior and surprising high UV photoresponse ($1350AW^{-1}$), which is two or three orders magnitude larger than reported GaN UV photodetector ($0.2\sim20AW^{-1}$). Such high photoresponse mainly originates from the introduction of ultrathin two-dimensional (2D) insulating h-BN layer, which behaves as the tunneling layer for holes produced in ZnO and the blocking layer for holes in graphene. The graphene/h-BN/ZnO heterostructure should be a novel and representative 2D heterostructure for improving the performance of 2D materials/Semiconductor heterostructure based optoelectronic devices.

OCIS codes: (040.5160) Photodetectors; (160.0160) Materials.

Rerences and links

1. K. S. Novoselov, V. I. Fal'ko, L. Colombo, P. R. Gellert, M. G. Schwab, and K. Kim, "A roadmap for graphene," Nature **490**(7419), 192–200 (2012).
2. A. H. Castro Neto, F. Guinea, N. M. R. Peres, K. S. Novoselov, and A. K. Geim, "The electronic properties of graphene," Rev. Mod. Phys. **81**(1), 109–162 (2009).
3. A. A. Balandin, S. Ghosh, W. Bao, I. Calizo, D. Teweldebrhan, F. Miao, and C. N. Lau, "Superior Thermal Conductivity of Single-Layer Graphene," Nano Lett. **8**(3), 902–907 (2008).
4. W. Cai, Y. Zhu, X. Li, R. D. Piner, and R. S. Ruoff, "Large area few-layer graphene/graphite films as transparent thin conducting electrodes," Appl. Phys. Lett. **95**(12), 123115 (2009).
5. T. Cohen-Karni, Q. Qing, Q. Li, Y. Fang, and C. M. Lieber, "Graphene and nanowire transistors for cellular interfaces and electrical recording," Nano Lett. **10**(3), 1098–1102 (2010).
6. Y. Zhu, S. Murali, W. Cai, X. Li, J. W. Suk, J. R. Potts, and R. S. Ruoff, "Graphene and graphene oxide: synthesis, properties, and applications," Adv. Mater. **22**(35), 3906–3924 (2010).
7. T. J. Echtermeyer, L. Britnell, P. K. Jasnos, A. Lombardo, R. V. Gorbachev, A. N. Grigorenko, A. K. Geim, A. C. Ferrari, and K. S. Novoselov, "Strong plasmonic enhancement of photovoltage in graphene," Nat. Commun. **2**, 458 (2011).
8. F. H. Koppens, T. Mueller, P. Avouris, A. C. Ferrari, M. S. Vitiello, and M. Polini, "Photodetectors based on graphene, other two-dimensional materials and hybrid systems," Nat. Nanotechnol. **9**(10), 780–793 (2014).
9. X. An, F. Liu, Y. J. Jung, and S. Kar, "Tunable graphene-silicon heterojunctions for ultrasensitive photodetection," Nano Lett. **13**(3), 909–916 (2013).
10. Q. Xu, Q. Cheng, J. Zhong, W. Cai, Z. Zhang, Z. Wu, and F. Zhang, "A metal-semiconductor-metal detector based on ZnO nanowires grown on a graphene layer," Nanotechnology **25**(5), 055501 (2014).
11. H. Zhong, K. Xu, Z. Liu, G. Xu, L. Shi, Y. Fan, J. Wang, G. Ren, and H. Yang, "Charge transport mechanisms of graphene/semiconductor Schottky barriers: A theoretical and experimental study," J. Appl. Phys. **115**, 013701 (2014).
12. A. K. Geim and I. V. Grigorieva, "Van der Waals heterostructures," Nature **499**(7459), 419–425 (2013).

#236116 Received 12 Mar 2015; revised 28 May 2015; accepted 29 May 2015; published 14 Jul 2015

13. M. Chhowalla, H. S. Shin, G. Eda, L. J. Li, K. P. Loh, and H. Zhang, "The chemistry of two-dimensional layered transition metal dichalcogenide nanosheets," Nat. Chem. **5**(4), 263–275 (2013).
14. K. F. Mak, C. Lee, J. Hone, J. Shan, and T. F. Heinz, "Atomically Thin MoS_2: A New Direct-Gap Semiconductor," Phys. Rev. Lett. **105**(13), 136805 (2010).
15. L. Song, L. Ci, H. Lu, P. B. Sorokin, C. Jin, J. Ni, A. G. Kvashnin, D. G. Kvashnin, J. Lou, B. I. Yakobson, and P. M. Ajayan, "Large scale growth and characterization of atomic hexagonal boron nitride layers," Nano Lett. **10**(8), 3209–3215 (2010).
16. K. K. Kim, S. M. Kim, and Y. H. Lee, "A new horizon for hexagonal boron nitride film," J. Korean Phys. Soc. **64**(10), 1605–1616 (2014).
17. C. R. D. Inanc Meric, Nicholas Petrone, Lei Wang, James Hone,Philip Kim, and Kenneth L. Shepard, "Graphene Field-EffectTransistors Based on Boron–Nitride Dielectrics," Proceedings of the IEEE (2013).
18. U. Özgür, Y. I. Alivov, C. Liu, A. Teke, M. A. Reshchikov, S. Doğan, V. Avrutin, S.-J. Cho, and H. Morkoç, "A comprehensive review of ZnO materials and devices," J. Appl. Phys. **98**(4), 041301 (2005).
19. Y. Ye, L. Gan, L. Dai, H. Meng, F. Wei, Y. Dai, Z. J. Shi, B. Yu, X. F. Guo, and G. G. Qin, "Multicolor graphene nanoribbon/semiconductor nanowire heterojunction light-emitting diodes," J. Mater. Chem. **21**(32), 11760–11763 (2011).
20. M. H. Huang, S. Mao, H. Feick, H. Yan, Y. Wu, H. Kind, E. Weber, R. Russo, and P. Yang, "Room-temperature ultraviolet nanowire nanolasers," Science **292**(5523), 1897–1899 (2001).
21. M. Law, L. E. Greene, J. C. Johnson, R. Saykally, and P. Yang, "Nanowire dye-sensitized solar cells," Nat. Mater. **4**(6), 455–459 (2005).
22. R. Yan, D. Gargas, and P. Yang, "Nanowire photonics," Nat. Photonics **3**(10), 569–576 (2009).
23. Y. Q. Bie, Z. M. Liao, H. Z. Zhang, G. R. Li, Y. Ye, Y. B. Zhou, J. Xu, Z. X. Qin, L. Dai, and D. P. Yu, "Self-powered, ultrafast, visible-blind UV detection and optical logical operation based on ZnO/GaN nanoscale p-n junctions," Adv. Mater. **23**(5), 649–653 (2011).
24. D. Shao, H. Sun, G. Xin, J. Lian, and S. Sawyer, "High quality ZnO–TiO2 core–shell nanowires for efficient ultraviolet sensing," Appl. Surf. Sci. **314**, 872–876 (2014).
25. L. Su, Q. Zhang, T. Wu, M. Chen, Y. Su, Y. Zhu, R. Xiang, X. Gui, and Z. Tang, "High-performance zero-bias ultraviolet photodetector based on p-GaN/n-ZnO heterojunction," Appl. Phys. Lett. **105**(7), 072106 (2014).
26. S. S. Lin, J. I. Hong, J. H. Song, Y. Zhu, H. P. He, Z. Xu, Y. G. Wei, Y. Ding, R. L. Snyder, and Z. L. Wang, "Phosphorus Doped Zn1-xMgxO Nanowire Arrays," Nano Lett. **9**(11), 3877–3882 (2009).
27. X. Q. Li, P. Wang, H. K. Zhong, Z. Q. Wu, H. S. Chen, C. Liu, and S. S. Lin, "High performance solar cells based on graphene-GaAs heterostructures," http://arxiv.org/abs/1409.3500 (2014).
28. S. Li, M. S. Toprak, Y. S. Jo, J. Dobson, D. K. Kim, and M. Muhammed, "Bulk Synthesis of Transparent and Homogeneous Polymeric Hybrid Materials with ZnO Quantum Dots and PMMA," Adv. Mater. **19**(24), 4347–4352 (2007).
29. M. Wang, S. K. Jang, W. J. Jang, M. Kim, S. Y. Park, S. W. Kim, S. J. Kahng, J. Y. Choi, R. S. Ruoff, Y. J. Song, and S. Lee, "A platform for large-scale graphene electronics--CVD growth of single-layer graphene on CVD-grown hexagonal boron nitride," Adv. Mater. **25**(19), 2746–2752 (2013).
30. H. I. Rasool, E. B. Song, M. J. Allen, J. K. Wassei, R. B. Kaner, K. L. Wang, B. H. Weiller, and J. K. Gimzewski, "Continuity of graphene on polycrystalline copper," Nano Lett. **11**(1), 251–256 (2011).
31. Y.-J. Yu, Y. Zhao, S. Ryu, L. E. Brus, K. S. Kim, and P. Kim, "Tuning the Graphene Work Function by Electric Field Effect," Nano Lett. **9**(10), 3430–3434 (2009).
32. D.-K. Hwang, S.-H. Kang, J.-H. Lim, E.-J. Yang, J.-Y. Oh, J.-H. Yang, and S.-J. Park, "p-ZnO/n-GaN heterostructure ZnO light-emitting diodes," Appl. Phys. Lett. **86**(22), 222101 (2005).
33. S. S. Lin, B. G. Chen, W. Xiong, Y. Yang, H. P. He, and J. Luo, "Negative thermal quenching of photoluminescence in zinc oxide nanowire-core/graphene-shell complexes," Opt. Express **20**(Suppl 5), A706–A712 (2012).
34. K. Keem, H. Kim, G.-T. Kim, J. S. Lee, B. Min, K. Cho, M.-Y. Sung, and S. Kim, "Photocurrent in ZnO nanowires grown from Au electrodes," Appl. Phys. Lett. **84**(22), 4376 (2004).
35. M. R. M. Atalla, Z. Y. Jiang, J. Liu, L. Wang, S. Ashok, and J. Xu, "Modeling the spectral responsivity of ultraviolet GaN Schottky barrier photodetectors under reverse bias," J. Appl. Phys. **117**(13), 134503 (2015).
36. M.-L. Lee, T. S. Mue, F. W. Huang, J. H. Yang, and J. K. Sheu, "High-performance GaN metal-insulator-semiconductor ultraviolet photodetectors using gallium oxide as gate layer," Opt. Express **19**(13), 12658–12663 (2011).
37. K. H. Lee, P. C. Chang, S. J. Chang, and S. L. Wu, "GaN-based Schottky barrier ultraviolet photodetector with a 5-pair AlGaN-GaN intermediate layer," Phys. Status Solidi **209**(3), 579–584 (2012).
38. H.-Y. Liu, W.-C. Hsu, B.-Y. Chou, Y.-H. Wang, W.-C. Sun, S.-Y. Wei, S.-M. Yu, and M.-H. Chiang, "Growing Al2O3 by Ultrasonic Spray Pyrolysis for Al2O3/AlGaN/GaN Metal-Insulator-Semiconductor Ultraviolet Photodetectors," IEEE Trans. Electron. Dev. **61**, 4062–4069 (2014).
39. J. Zhou, Y. Gu, Y. Hu, W. Mai, P. H. Yeh, G. Bao, A. K. Sood, D. L. Polla, and Z. L. Wang, "Gigantic enhancement in response and reset time of ZnO UV nanosensor by utilizing Schottky contact and surface functionalization," Appl. Phys. Lett. **94**(19), 191103 (2009).
40. C. Soci, A. Zhang, B. Xiang, S. A. Dayeh, D. P. R. Aplin, J. Park, X. Y. Bao, Y. H. Lo, and D. Wang, "ZnO nanowire UV photodetectors with high internal gain," Nano Lett. **7**(4), 1003–1009 (2007).
41. W. Park, G. Jo, W. K. Hong, J. Yoon, M. Choe, S. Lee, Y. Ji, G. Kim, Y. H. Kahng, K. Lee, D. Wang, and T.

#236116 Received 12 Mar 2015; revised 28 May 2015; accepted 29 May 2015; published 14 Jul 2015

Lee, "Enhancement in the photodetection of ZnO nanowires by introducing surface-roughness-induced traps," Nanotechnology **22**(20), 205204 (2011).
42. D. Lin, H. Wu, W. Zhang, H. Li, and W. Pan, "Enhanced UV photoresponse from heterostructured Ag–ZnO nanowires," Appl. Phys. Lett. **94**(17), 172103 (2009).
43. S. Sahoo, S. K. Barik, A. P. S. Gaur, M. Correa, G. Singh, R. K. Katiyar, V. S. Puli, J. Liriano, and R. S. Katiyar, "Microwave Assisted Synthesis of ZnO Nano-Sheets and Their Application in UV-Detector," ECS J. Solid State Sci. Technol. **1**(6), Q140–Q143 (2012).
44. K. W. Liu, M. Sakurai, M. Y. Liao, and M. Aono, "Giant Improvement of the Performance of ZnO Nanowire Photodetectors by Au Nanoparticles," J. Phys. Chem. C **114**(46), 19835–19839 (2010).
45. H. von Wenckstern, G. Biehne, R. A. Rahman, H. Hochmuth, M. Lorenz, and M. Grundmann, "Mean barrier height of Pd Schottky contacts on ZnO thin films," Appl. Phys. Lett. **88**(9), 092102 (2006).

1. Introduction

Graphene, the first discovered two dimensional material, has aroused great interest since discovered in 2004, which exhibits extremely high carrier mobility, excellent thermal conductivity and mechanical flexibility [1–3]. With these unique properties, graphene has great potential in the next generation of electronic and optoelectronic devices [4–6]. When graphene is used as light-to-current converter layer, the photocurrent responsibility is typically limited within 130mA/W for the low optical absorption of graphene [7, 8]. Integrating graphene with bulk semiconductor should improve the photo responsibility of devices [9, 10]. The interface between graphene and semiconductor, which influences the junction barrier height, determines the performance of Schottky diodes [9]. As graphene is atomic thin and the density states near the Dirac point of electronic band structure of graphene is low, the carriers transfer between graphene and semiconductor will decrease the barrier height of this Schottky diode, which limits the performance of graphene-semiconductor based Schottky diode [11]. The introduction of insulating layer between graphene and bulk semiconductor may overcome this problem. In parallel with the development of graphene/bulk semiconductor heterostructure, van der Waals heterostructure based on the stacking of two-dimensional (2D) materials have received much attention for their extraordinary physical properties [12]. Among those potential semiconductor, 2D TMDs such as MoS_2, WS_2 have been the current focus of the 2D community [13]. However, the limited band gap commonly less than 2.0 eV is not effective to inhibit the carrier transfer between graphene and bulk semiconductor [14].

The hexagonal boron-nitride (h-BN) is a III-V compound insulator with wide band gap of 5.97eV, which has outstanding chemical stability, high transparency and flexibility [15, 16] and can be used as a dielectric layer in flexible electronics [17]. Although not reported yet, h-BN could be inserted between graphene and bulk semiconductor as the barrier layer, which will inhibit the static charge transfer between graphene and bulk semiconductor, resulting a higher Fermi level difference between those two sides.

On the other hand, bulk semiconductor is an important part of the graphene-semiconductor based Schottky diode, which should be well designed and chosen for better performance. ZnO is a semiconductor with direct wide band-gap (3.3eV at 300K), high chemical stability and large exciton binding energy (60meV) which is promising for light-emitting-diodes, laser diodes, and ultraviolet (UV) photodetectors [18–26]. Herein, we designed a novel photodetector based on graphene/ZnO single crystal heterostructure sandwiched with different layers of h-BN and the results show that h-BN layer can largely improve the rectification capability of graphene/ZnO interface, which leads to an enhanced photoresponse of the heterostructure.

2. Graphene/h-BN/ZnO van der Waals Schottky diode

The single side polished ZnO single crystal substrates with carrier concentration of 10^{16} cm^{-3} bought from MTI Corporation were used in the experiment. Both the graphene layer and the h-BN layers (5 atom layers thick) were grown by chemical vapor deposition (CVD) method [15, 27]. Ni/Au (5nm/50nm) electrodes were deposited on rough side of the ZnO substrate for

#236116 Received 12 Mar 2015; revised 28 May 2015; accepted 29 May 2015; published 14 Jul 2015

achieving ohmic contact. The PMMA supported CVD grown h-BN layers were transferred onto the polished side of ZnO then immersed in acetone and isopropanol in turn for half an hour to remove the PMMA. The polyimide type deposited with Ni/Au (5nm/50nm) electrode was placed on the h-BN layer. Then, PMMA supported CVD grown monolayer graphene (MLG) was transferred onto the h-BN layers and the electrodes. Graphene naturally forms the ohmic contact with Ni/Au electrode after transferring. The device area is about 25mm^2 (5mm × 5mm). Here the PMMA layer was not dissolved as it is highly transparent to UV light and the PMMA layer can protect the interface of MLG/h-BN/ZnO heterostructure from the environment [28]. Transmission electron microscope (TEM) characterization of h-BN was carried out in a Technai F-20 system and Raman spectra were measured by a Reinishaw system with an excitation laser of 532 nm. Schematic illustration and photodetector test of the MLG/h-BN /ZnO structure are shown in Fig. 1 (a) and Fig. 1(b), respectively. A commercial UV light of 365 nm was used as the illumination source for the photodetector test, which is carried out under the dark environment and the power density was measured by SUSS MicroTec UV-Optometer.

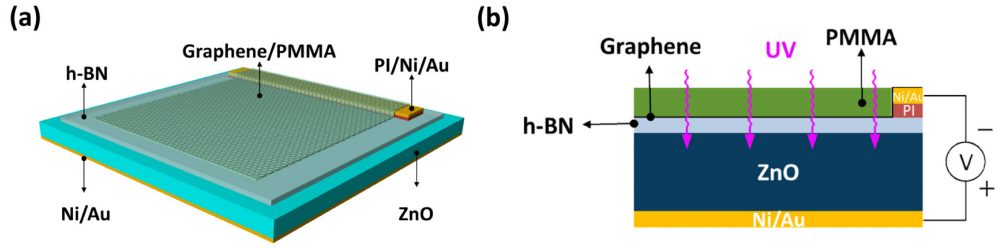

Fig. 1. Schematic diagram and cross-section of the MLG/h-BN /ZnO structure.

3. Results and discussion

For revealing the thickness of h-BN, we transfer the h-BN to copper grid for TEM characterizations. Figure 2(a) show the low-magnification TEM image of h-BN and the inset shows the diffractions pattern of h-BN, where five dots corresponding to $(1\bar{1}20)$ lattice plane can be found, indicating the h-BN could be five or six layers thick. The high-resolution TEM image of the edge of the h-BN is shown in Fig. 2(b), which clearly shows that our h-BN has a thickness of five layers. We transferred the identical h-BN layers and graphene used in the device onto the Si/SiO_2 substrate for Raman measurements. The Raman feature of graphene/h-BN heterostructure is shown in Fig. 2(c), where the peak near the 1366cm^{-1} due to the E_{2g} vibrational mode of h-BN indicates the existence of h-BN layers [29]. Figure 2(c) also shows the Raman feature of monolayer graphene transferred onto the Si/SiO_2 substrate. The high 2D/G ratio larger than two and the weak D peak indicate high-quality single layer graphene [30].

#236116 Received 12 Mar 2015; revised 28 May 2015; accepted 29 May 2015; published 14 Jul 2015

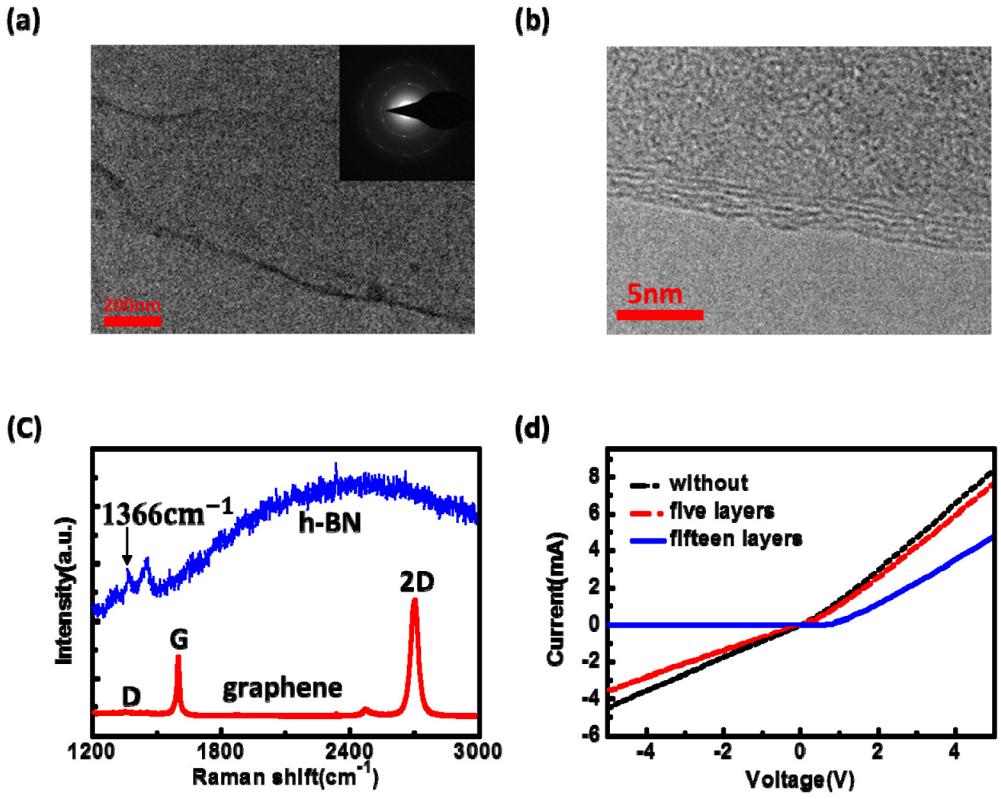

Fig. 2. (a) TEM image of the h-BN and inset shows the electron diffractions pattern of h-BN (b) High-resolution TEM image of the edge of h-BN (c) Raman feature of graphene/h-BN heterostructure (d) the I-V curves of MLG/ZnO Schottky diode sandwiched with different layers of h-BN.

Although Schottky contact can be formed between graphene and ZnO due to the difference of their work function (0.22eV) theoretically [31, 32], the charge transfer between graphene and ZnO is severe according to our previous report [33]. This charge transfer leads to an extraordinary large leak current of graphene-ZnO heterostructure, as shown in Fig. 2(d). The dark line, red line and blue line represent the current-voltage (I-V) characteristics of MLG/ZnO, MLG/five layers h-BN/ZnO and MLG/fifteen layers h-BN/ZnO diode, respectively. To MLG/ZnO device, we observed a large reverse leakage current, about 4.5mA at −5V and the I-V curve reveals only weak rectifying behavior. This result is mainly caused by the charge transfer between graphene and ZnO as well as the existence of impurities introduced during transfer process. Compared with MLG/ZnO device, the rectifying effect of MLG/five layers h-BN/ZnO device is improved slightly. When the number of h-BN layers increases to fifteen, the device shows a significant improved rectifying behavior with a turn on voltage of ~1V. The best forward and reverse current ratio at V is ~10^3. At forward bias, the resistance of MLG/ZnO and MLG/fifteen layers h-BN/ZnO is about 540Ω and 800Ω, respectively. The increase of resistance is caused by the insulation of h-BN layer.

The MLG/fifteen layers h-BN/ZnO device shows distinctive rectifying behavior. While exposed to 365 nm UV light irradiation, the Schottky barrier disappears [34]. Figure 3(a) shows the I-V curves of the MLG/three layers h-BN/ZnO device under different power density UV illumination. The photoresponse can reach 1350AW^{-1} at −5V when the incident power density is 5μW cm^{-2}. This responsibility is three orders of magnitude larger than traditional GaN photodetectors (<0.2A/W) [25, 35–38]. Such high responsibility can be

#236116 Received 12 Mar 2015; revised 28 May 2015; accepted 29 May 2015; published 14 Jul 2015

attributed to high quantum efficiency of ZnO and the sandwiched graphene/h-BN/ZnO structure. It is noteworthy that graphene/ZnO heterostructure with h-BN has no UV photoresponse. When the Schottky junction is applied with reverse bias, the mainly voltage drop occurs at the depletion region in ZnO. When the junction is illuminated with 365nm UV light, the photon-generated carriers are separated quickly by the strong local electric field, hence reduce the electron-hole recombination rates [39]. On the other hand, there are few recombination centers in the single crystal ZnO. Those two factors increase the carrier life time and resulting a large photoconductive gain [40].It is obvious that photocurrent increases with the increasing of power density of UV illumination and when power density increases to 70μW cm^{-2}, the photocurrent starts to saturate, as shown in Fig. 3(b). Figure 3(c) shows the time dependence of the photocurrent when the UV light is switching on/off in a cycle of 30 seconds. Upon exposing UV light, the photocurrent increases rapidly, this period continues for 1 second, approximately. Then the photocurrent shows a slow increase. When the UV light is turned off, the photocurrent decreases rapidly then slowly. The fast decrease process continues for about 5 seconds then the photocurrent decreases slowly. The increase time and decrease time are faster than many reported ZnO based UV photodetector (from several seconds to several minutes) [41, 42]. Figure 3(d) shows the behavior of photocurrent decay in detail. By fitting the experimental data, the decay process follows a function consist of two exponential decay functions. While the form of the function is

$$I_{ph} - I_{dark} = A_1 \exp(-\frac{t - t_{off}}{\tau_1}) + A_2 \exp(-\frac{t - t_{off}}{\tau_2}) \quad (1)$$

τ_1 represents the time constant of photo generated electrons and holes recombination process. Fitted results of τ_1 and τ_2 are 0.84s and 5.26s, respectively. τ_2 is a slow response process may be associated with the oxygen absorption and desorption process in the interface of h-BN/ZnO [43, 44].

#236116 Received 12 Mar 2015; revised 28 May 2015; accepted 29 May 2015; published 14 Jul 2015

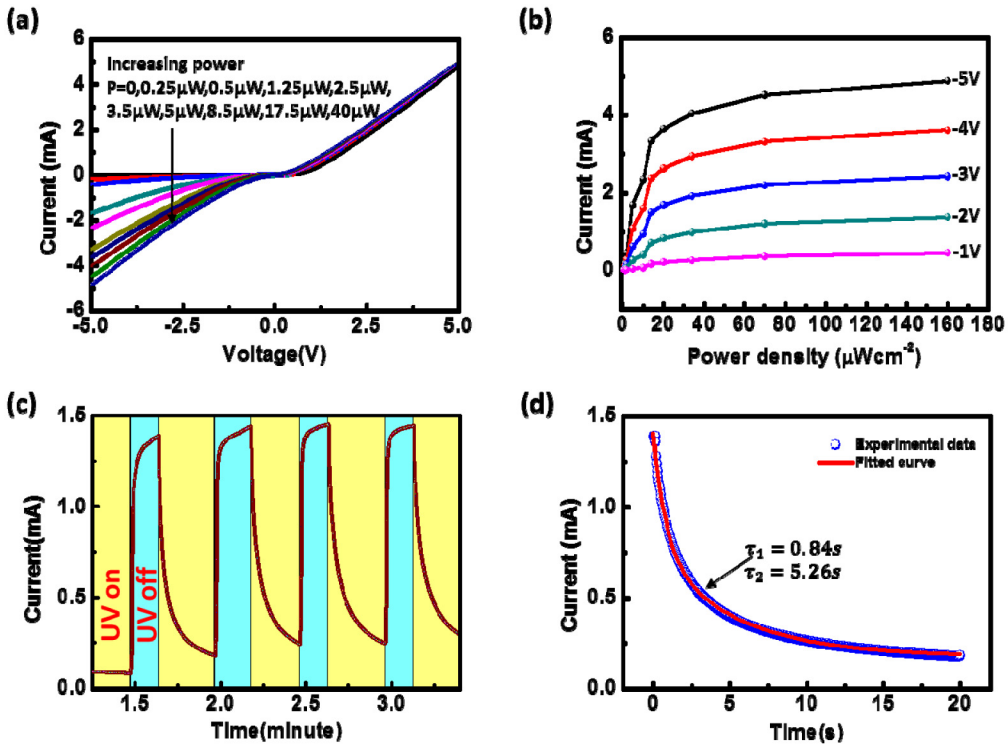

Fig. 3. (a) I-V characteristics of the graphene/three layers BN/ZnO UV detector under illumination of 365nm UV light and the power density of UV ranging from 0 to 160μW cm^{-2} (b) Varation of the photocurrent with the intensity of UV illumination (c)Time dependence of photocurrent when switching UV light on and off at a cycle of 30s. The reverse bias is 1V. (d)Photocurrent decay process and the fitted line, reverse bias is 1V.

The energy-band diagrams of graphene/h-BN/ZnO device under reverse bias are shown in Fig. 4.In fact, the I-V characteristics of the graphene/h-BN/ZnO heterostructure can be described in following equations:

$$J = T_p J_0 (\exp \frac{qv}{nk_B T} - 1) \tag{2}$$

T is the absolute temperature, n is the junction ideality factor, k_B represents for the Boltzmann constant. T_p is the tunneling probability, which can be described as below:

$$T_p = \exp(-2 \frac{\sqrt{2m^* q \Phi_{barrier}}}{\frac{h}{2\pi}} d) \tag{3}$$

m* is the effective mass of the tunneling carrier, d is the thickness of insulating layer, h represents for Plank constant. J_0 is the junction saturation current density,

$$J_0 = A^* T^2 \exp(-\frac{q\Phi_{barrier}}{k_B T}) \tag{4}$$

A* is the effective Richardson's constant of ZnO ($32 Acm^{-2} K^{-2}$) [45]. The $\Phi_{barrier}$ calculated here is about 0.65eV while the $\Phi_{barrier}$ between graphene and ZnO is 0.22eV in theory. In

#236116 Received 12 Mar 2015; revised 28 May 2015; accepted 29 May 2015; published 14 Jul 2015

dark environment, the higher barrier formed between graphene and h-BN can suppress the tunneling of electrons from the valence band of graphene to the conduction band of ZnO at reverse bias. The holes are minority carrier in ZnO and the concentration of holes are several magnitude smaller than electrons. Although holes in ZnO can tunnel through the h-BN layer under the action of applied electric field, the hole current is very small, as shown if Fig. 4(a). While under UV illumination, the photo-generated holes will inject into graphene under the applied electric field, this process leads to a large increase of reverse current, as shown in Fig. 4(b). Without the BN layer, although the photo-generated holes can transfer from ZnO to graphene layer, however, the holes will recombine with the electrons or defect levels in ZnO immediately, which leads the negligible photoresponse behavior of Graphene/ZnO heterostructure. This physical picture is in agreement with our previous temperature dependent photoluminescence study of ZnO-core/Graphene-shell structure [33].

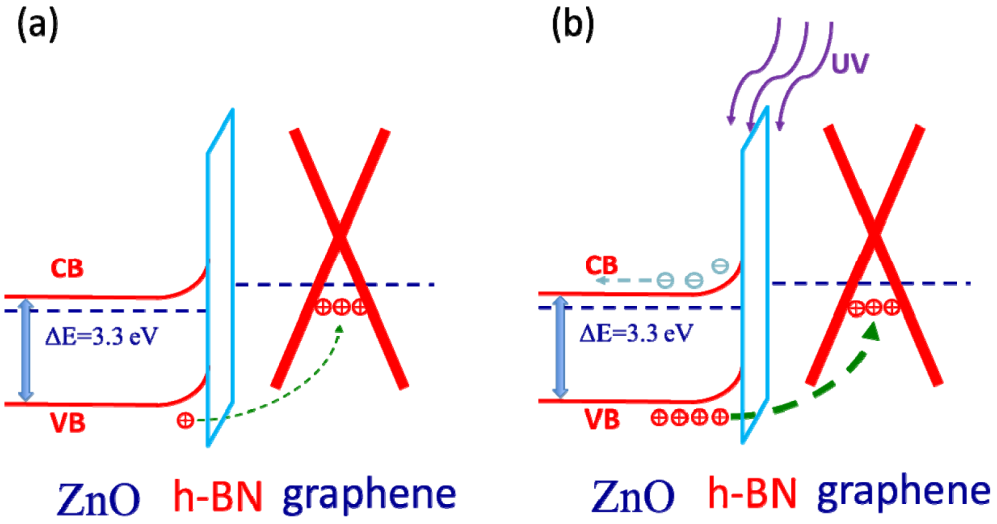

Fig. 4. The energy-band diagrams of graphene/h-BN/ZnO device (a) under reverse bias and dark (b) under reverse bias and UV illumination.

4. Conclusion

In summary, we have demonstrated a novel graphene/h-BN/ZnO tunneling UV photodetector. The photocurrent response of the detector can reach 1350AW^{-1}, which is four orders of magnitude larger than that of traditional GaN photodetectors. Such high photoresponse is attributed to the introduction of h-BN layer. This graphene/h-BN/ZnO device may be promising candidate for weak signal UV detection.

Acknowledgments

S. S. Lin thanks the support from the National Science Foundation of China (51202216) and X. Q. Li thanks the support from the Postdoctoral Science Foundation of China (111400-X91305).